Res Chem Intermed
DOI 10.1007/s11164-016-2426-x

Syntheses and crystal structures of two self-assembled dizinc(II) helicates with novel hydrazone linked polypyridyl ligands

Hsien-Chang Kao[1] · **Yi-Chun Wang**[1] · **Wen-Jwu Wang**[1]

Received: 18 December 2014 / Accepted: 18 February 2015

Abstract The rationally designed polydentate ligands, $\mathbf{L^1}$ and $\mathbf{L^2}$, based on the pyridinyl moiety and the hydrazone fragment have been synthesized to coordinate zinc(II) ions. We utilize pyridine as a rigid core connecting two bipyridines as ligand building blocks with a hydrozone linker for the $\mathbf{L^1}$. The $\mathbf{L^2}$ has a reversed design in which a bipyridine was used as a hinging-available building block of the ligand core, connecting two pyridazine arms with a hydrazone linker. Two novel helical dizinc(II) complexes were obtained by the reaction of $\mathbf{L^1}$ and $\mathbf{L^2}$ with zinc(II) perchlorate in acetonitrile. The structures of both helicates were confirmed by X-ray diffractometry. Single-stranded helicate $\mathbf{Zn_2L^1}$ contains two zinc ions bridged by an oxygen atom. Except for the $\mathbf{L^2}$ ligand, no other bridging species were found between the two zinc ions in the double-stranded helicate $\mathbf{Zn_2L^2_2}$. The self-assembling process of helicate $\mathbf{Zn_2L^1}$ in solution state was studied by UV–Vis spectrometric titration experiments. The stepwise formation constants imply a slightly positive cooperative behavior for the formation of helicates.

Keywords Supramolecular chemistry · Double-strand · Helicates · Dizinc complex

Introduction

Self-assembly supramolecules have received considerable attention during the last few decades [1–7] because of the important role played by supramolecules for applications of catalysts, medicines, sensors, devices, and functional materials [8–11]. The design and synthesis of inorganic helical complexes involving non-covalent interactions, such as metal–ligand coordination bonding, hydrogen

---

✉ Wen-Jwu Wang
wjw@mail.tku.edu.tw

[1] Department of Chemistry, Tamkang University, Tamsui, New Taipei City 25137, Taiwan

bonding, charge transfer interaction, hydrophobic interaction, and metal–metal interaction has attracted extensive interest. The stereochemistry of metallo-supramolecules can be built up through rational design of characteristic ligands as well as metal ions with preferred stereochemistry [12–15]. Based on the choice of the coordination sphere with variation of the donor ligand, various single- and double-stranded helical architectures can be feasible.

The selection of suitable organic ligands is crucial for constructing extended metal complexes. N-heterocyclic ligands have been frequently employed due to their ability to engage in diverse coordinations. Two N-heterocycles linked by suitable spacers have been proven to lead to a great structural diversity among complexes [16–19]. Various spacers have been used to connect polypyridinyl and other components, which is the key factor to control the resulting structure of the complex [20, 21]. Furthermore, the preparation and modification of those ligands in high yield is remarkable. In spite of the dipyridinyl ligand and its analogue being studied by a number of researchers, studies of the hydrazone group as linkers are relatively rare. The hydrazone group has a twistable N–N single bond that is employed to change between a cisnoid and a transnoid form. The polypyridinyl–hydrazone compounds are versatile N-donor ligands since the flexible nature of the ligands frequently fitted diverse requirements.

From the other point of view, transition metal ions play a key role in the formation of coordination compounds with a suitable coordination number and geometry [22, 23]. Zn(II) ions can assume multiple coordination geometries ranging from regular or distorted tetrahedral to trigonal bipyramidal, square pyramidal, and octahedral geometries of different coordination numbers. Meanwhile, the kinetic lability of coordinated ligands is also responsible for their wide utility within biological and photochemical systems [24–27].

Following these criteria, novel a multi-dentate ligand Py-Me-(Bpy)$_2$ (**L^1**) and a Bpy-(Me-Pz)$_2$ (**L^2**) were designed and synthesized. **L^1** has a central pyridine core and two bipyridyl arms. **L^2**, on the other hand, has a bipyridyl core and two pyrazine arms. The core and the arms are connected by a hydrozone linker on each. Previously, we have shown that the ligand **L^2** formed a double helix structure with an octahedral geometry to metal ions such as Ni(II) and Cu(II), through a self-assembly process. We now turn our focus to Zn(II), which is one of the most interesting transition metals due to its variable coordination ability. We report herein the synthesis, crystal structure, and spectroscopic characterization of the self-assembled zinc helicate complexes.

Experimental

All commercially available chemicals were of reagent grade and used without further purification, unless otherwise stated. Diethyl ether was distilled from sodium benzophenone ketyl immediately prior to use. Dichloromethane was distilled over calcium hydride. All solvents were of HPLC grade. The electrospray ionization mass spectral (ESI–MS) measurements were carried out on a LCQ (Finnegan MAT, USA) using methanol as the mobile phase. The samples for ESI–MS measurements were prepared by redissolving the final isolated compounds in methanol. 1H NMR spectra were measured in $CDCl_3$ with a Bruker AC300 300 MHz spectrometer at room temperature. Spectrophotometric titrations were performed with a Shimadzu UV-1601 UV–visible spectrophotometer connected to an external computer.

Synthesis of the ligand and complex

1-Methyl-2,2′-bipyridinium Iodide, (MBPI)

A 14 mL methyl iodide solution was added to a 35 mL nitrobenzene solution of 2,2′-bipyridine (127.99 mmol, 19.99 g). The mixture was placed at room temperature for 2 weeks and the yellow crystals were generated, which were then collected by filtration and air-dried. The yellow crystals were recrystallized by *n*-hexane to give 30 g (120.3 mmol) of the product.

1-Methyl-2,2′-bipyridine-6-one, (MBPO)

A 10 mL aqua solution of MBPI (4.01 g, 13.00 mmol) and a 9 mL aqua solution of sodium hydroxide (5.01 g, 125.25 mmol) were added dropwise into 26 mL potassium hexacyanoferrate(III) (10.49 g, 30.99 mmol) in an ice bath. The deep brown mixture was stirred for 1 h, then extracted by dichloromethane. The product was treated using a column of silica gel. The yellow solution was concentrated and dried to get the brown product (0.97 g, 5.2 mmol).

6-Chloro-2,2′-bipyridine, (CBP)

A 9.8 mL phosphoryl chloride solution was added into a mixture of MBPO (0.99 g, 5.32 mmol) and phosphorus pentachloride (0.93 g, 4.46 mmol). The brown mixture was refluxed for 1 day and became a deep brown color. The unreacted phosphoryl chloride was removed and then put into an ice bath. Then 100 mL of ice water was added and the precipitate was filtered out. The solution was slowly added into ammonium hydroxide until the pH reached 7. The white precipitate was generated and then collected and recrystallized by dichloromethane in a 76 % yield.

^1H NMR (300 MHz, $CDCl_3$) δ (ppm) 8.66 (*d*, 1H, $J = 2.3$ Hz, Cl-Bipy-*H*), 8.39 (*d*, 1H, $J = 4.0$ Hz, Cl-Bipy-*H*), 8.34 (*d*, 1H, $J = 3.8$ Hz, Bipy-*H*), 7.82 (*t*, 1H, $J = 3.8$ Hz, Bipy-*H*), 7.77 (*t*, 1H, $J = 3.8$ Hz, Bipy-*H*), 7.35 (*d*, 1H, $J = 3.8$ Hz, Bipy-*H*), 7.31 (*t*, 1H, $J = 7.7$ Hz, 1H, Cl-Bipy-*H*).

6-Hydrazine-2,2′-bipyridine, (HzBpy)

Hydrazine monohydrate (20 mL) and a few drops of methanol were added to CPB (2.01 g, 10.52 mmol), then set to reflux for 1 day under dry nitrogen with vigorous stirring. An additional 15 mL of hydrazine monohydrate was added after the solution became clear. The solution was then refluxed for one more day, after which the mixture was then extracted and recrystallized by dichloromethane to give 1.72 g

(88 % yield) of the product. Anal. Calcd for $C_{10}H_{10}N_4$: C, 64.50; H, 5.41; N, 30.09 Found. C 64.48, H 5.46, N 30.11.

^{1}H NMR (300 MHz, $CDCl_3$) δ (ppm) 8.66 (*d,* 1H, $J = 2.3$ Hz, Bipy-*H*), 8.29 (*d,* 1H, $J = 3.0$ Hz, Bipy-*H*), 7.80 (*d,* 1H, $J = 2.2$ Hz, Bipy-*H*), 7.75 (*t,* 2H, $J = 3.3$ Hz, Bipy-*H*), 7.62 (*t,* 1H, $J = 3.8$ Hz, NH-NH_2-Bipy-*H*), 7.26 (*t,* 1H, $J = 3.8$ Hz, NH-NH_2-Bipy-*H*), 6.75 (*d,* 1H, $J = 4.0$ Hz, NH-NH_2-Bipy-*H*), 3.68 (*s,* 1H, Bipy-*NH*).

2,6-Diacetylpyridine bis(2,2′-bipyridyl-6-hydrazone), (Py-Me-$(Bpy)_2$, L^1)

A 30 mL methanol solution of HzBpy (1.80 g, 9.67 mmol) was added to a 15 mL methanol solution of 2,6-diacetyl–pyridine (0.80 g, 4.9 mmol). The solution was set to reflux for 1 day, and the light yellow precipitate was generated. The precipitate was collected by filtration and washed with methanol and diethyl ether, then dried under vacuum to give 2.23 g (4.41 mmol, 90 % yield) of the product. Anal. Calcd for C_{29}H25N_9: C 69.72, H 5.04, N 25.23. Found. C 69.68, H 5.11, N 25.27.

^{1}H NMR (300 MHz, $CDCl_3$) δ (ppm) 8.70 (*d*, 1H, $J = 2.1$ Hz, Bipy-*H*), 8.28 (*d*, 1H, $J = 3.9$ Hz, Py-*H*), 8.10 (*d*, 1H, $J = 3.9$ Hz, C=N–NH-Bipy-*H*), 7.84 (*m*, 2.5 H, Py-*H,* Bipy-*H,* C=N–NH-Bipy-*H*), 7.72 (*t*, 1H, $J = 3.9$ Hz, Bipy-*H*), 7.52 (*d*, 1H, $J = 3.6$ Hz, C=N–NH-Bipy-*H*), 7.28 (*dd*, 1H, $J = 4.5$, 3.2 Hz, Bipy-*H*), 2.54 (*s*, 3H, *CH_3*).

$[Zn_2(Py\text{-}Me\text{-}(Bpy)_2)(OH)(CH_3CN)(H_2O)](ClO_4)_3$, ($Zn_2L^1$)

A 10 mL acetonitrile solution of $Zn(ClO_4)_2{\cdot}6\ H_2O$ (14.89 mg, 0.04 mmol) was added slowly into a 10 mL acetonitrile solution of $\mathbf{L^1}$ (10 mg, 0.02 mmol). The solution immediately turned light yellow. Toluene was diffused into the mixture and the yellow crystals were collected by filtration to give a product in 55 % yield. Anal. Calcd for $C_{44}Cl_4H_{40}N_{20}O_{16}Zn_2$: C 38.36, H 2.93, N 20.33. Found. C 38.19, H 3.06, N 20.32.

2,2′-Bipyridyl-6,6′-bis(2-acetylpyrazinohydrazone), (Bpy-$(Me\text{-}Pz)_2$, L^2)

The ligand $\mathbf{L^2}$ was synthesized following the procedure described in our previous paper [28, 29].

$[Zn_2(Bpy\text{-}(Me\text{-}Pz)_2)](ClO_4)_4$, ($Zn_2L^2_2$)

A 15 mL acetonitrile solution of $Zn(ClO_4)_2{\cdot}6\ H_2O$ (18.61 mg, 0.05 mmol) was added slowly into a 15 mL acetonitrile solution of $\mathbf{L^2}$ (19.89 mg, 0.05 mmol). The solution turned light yellow immediately. Toluene was diffused into the mixture, and the yellow crystals were collected by filtration to give a product in 55 % yield.

Anal. Calcd for $C_{44}Cl_4H_{40}N_{20}O_{16}Zn_2$: C 38.36, H 2.93, N 20.33. Found. C 38.19, H 3.06, N 20.32.

Crystal structure determination of complex Zn_2L^1, $Zn_2L^2_2$

Data were collected at 120 K on a Nonius KappaCCD area detector situated at the window of a rotating anode (λMo-k$_\alpha$ = 0.71073 Å). The structure was solved by direct methods, SHELXS-97, and refined using SHELXL-97 [30]. Hydrogen atoms

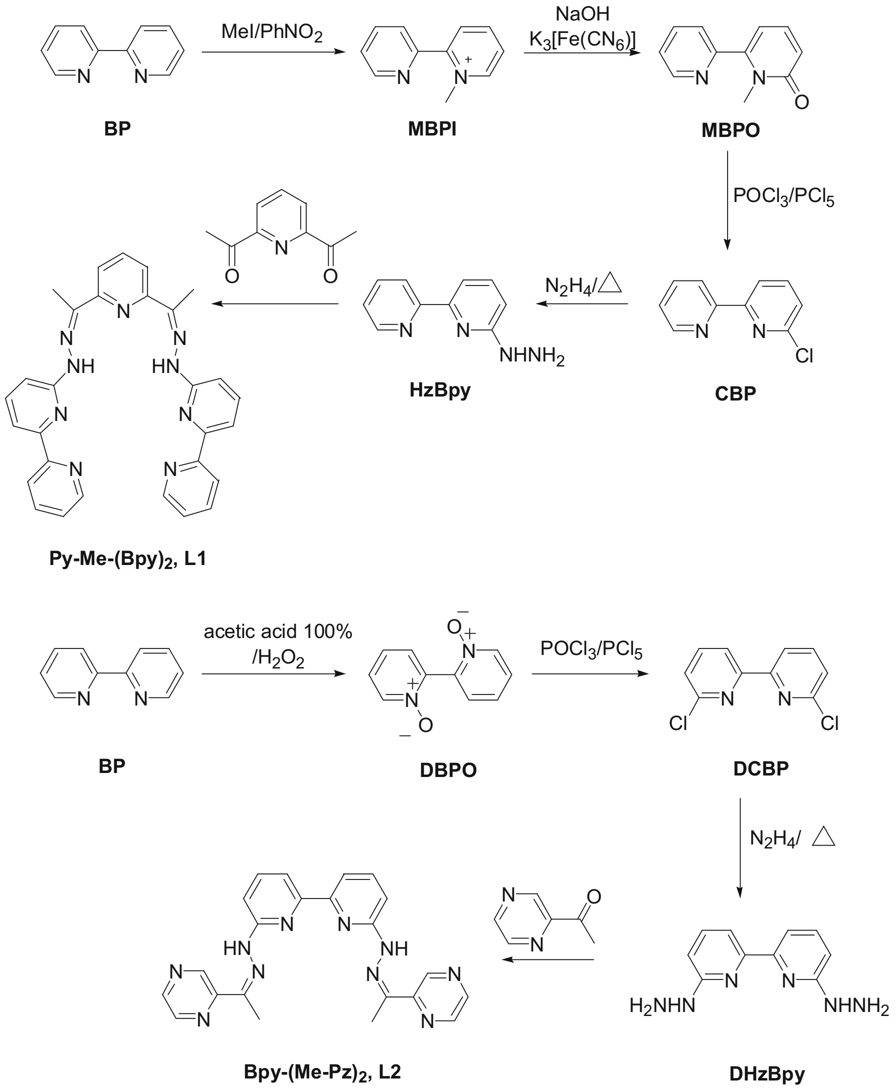

Scheme 1 Synthesis of ligands $\mathbf{L^1}$ and $\mathbf{L^2}$

were included in the refinement, but thermal parameters and geometry were constrained to ride on the atom to which they were bonded. The data were corrected for absorption effects using SADABS [31]. The perchlorate anions exhibited crystallographic and dynamic disorder in both Zn_2L1 and $Zn_2L^2_2$. $\mathbf{Zn_2L^1}$: C33H38Cl3N11O16Zn2, Monoclinic, $P2_1/n$, $a = 17.3644(4)$, $b = 10.3116(2)$, $c = 24.4661(8)$ Å, $\alpha = 90°$, $\beta = 92.7430(10)°$, $\gamma = 90°$, volume = 4375.75(19) Å^3, $Z = 4$, $D_c = 1.642$ Mg/m^3, $\theta_{max} = 25.03°$, 26,971 measured, 7644 unique ($R_{int} = 0.0844$) and 7644 ($I > 2\sigma(I)$) reflections, $R1$ (obs.) = 0.0610 and $wR2$ (all data) = 0.2023, $\rho_{max}/\rho_{min} = 1.122/-0.874$ eÅ^{-3}. $\mathbf{Zn_2L^2_2}$: C48H48Cl4N22O17Zn2, Monoclinic, $P2_1/n$, $a = 12.0256(13)$, $b = 21.274(2)$, $c = 24.059(3)$ Å, $\alpha = 90°$, $\beta = 103.280(2)°$, $\gamma = 90°$, volume = 5990.7(11) Å^3, $Z = 4$, $D_c = 1.636$ Mg/m^3, $\theta_{max} = 26.03°$, 33,578 measured, 11,766 unique ($R_{int} = 0.0457$) and 11,766 ($I > 2\sigma(I)$) reflections, $R1$ (obs.) = 0.0767 and $wR2$ (all data) = 0.1086, $\rho_{max}/\rho_{min} = 0.465/-0.508$ eÅ^{-3}.

Determination of formation constant

In a typical experiment, 100 mL of ligand $\mathbf{L^1}$ in acetonitrile/dichloromethane (1:1, v/v) solution (0.101 mM) was titrated with a concentration solution (ca. 4 equivalent) of the zinc(II) perchlorate hexahydrate in CH_3CN. Each addition of the salt solution (25 mL increments at 5 min intervals), was carried out by using a precision micropipette at 25 °C. The absorbance was recorded using a 1 cm quartz cell and then transferred to the computer. The spectral data were analyzed with the

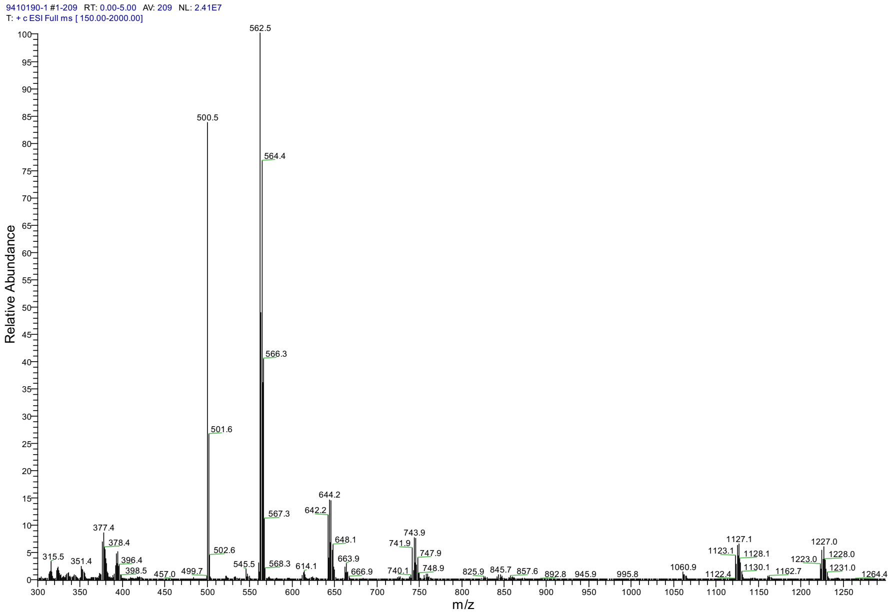

Fig. 1 ESI–MS spectrum of $\mathbf{Zn_2L^1}$ (0.2 mM) in methanol solution

Specfit program [32–35], by which the absorption and the stability constants of each species forming in equilibrium processes were obtained. The *Specfit* program uses factor analysis (which confirms the number of different absorbing species) to reduce the absorbance matrix and to extract the eigenvalue prior to the multiwavelength fit of the reduced data set according to the *Marquard* algorithm [36]·

Results and discussion

Synthesis

The synthesis of the precursor HzBpy is the key step for approving the ligand, according to Scheme 1. The ligand $\mathbf{L^1}$, pyridinyl as the central core and two bipyridinyls as the arms, were synthesized by the condensation of HzBpy and 2,6-diacetyl-pyridine. The ligand $\mathbf{L^2}$ was synthesized by a modified literature method. The stepwise addition of hydrazine to the reaction vessel is the key step for approving high yield to prepare the ligand $\mathbf{L^2}$. The free ligands $\mathbf{L^1}$ and $\mathbf{L^2}$ were then added into one equivalent $Zn(ClO_4)_2{\cdot}6H_2O$ in CH_3CN leading to the dinuclear single-stranded helical complex $\mathbf{Zn_2L^1}$ and dinuclear double-stranded helical complex $\mathbf{Zn_2L^2_2}$. The complex $\mathbf{Zn_2L^1}$ was characterized by ESI-Mass spectroscopy (Fig. 1), and the structure of $\mathbf{Zn_2L^1}$ and $\mathbf{Zn_2L^2_2}$ were characterized by X-ray crystallography.

Table 1 Selected bond lengths (Å) and angles[°] for $\mathbf{Zn_2L^1}$ and $\mathbf{Zn_2L^2_2}$

$\mathbf{Zn_2L^1}$			
Bond length			
Zn(1)–O(1)	1.909(4)	Zn(2)–O(1)	1.984(4)
Zn(1)–N(10)	2.031(6)	Zn(2)–O(2)	2.065(4)
Zn(1)–N(2)	2.040(5)	Zn(2)–N(8)	2.102(5)
Zn(1)–N(1)	2.163(5)	Zn(2)–N(6)	2.185(5)
Zn(1)–N(4)	2.273(5)	Zn(2)–N(9)	2.285(5)
Zn(2)–N(5)	2.335(5)		
Bond angle			
Zn(1)–O(1)–Zn(2)	126.5(2)	O(1)–Zn(2)–N(5)	87.39(16)
N(5)–Zn(2)–N(9)	141.15(18)	O(1)–Zn(2)–N(8)	102.66(17)
N(6)–Zn(2)–N(8)	74.1(2)	O(2)–Zn(2)–N(5)	78.23(17)
N(5)–Zn(2)–N(6)	71.12(18)	O(2)–Zn(2)–N(8)	106.80(19)
$\mathbf{Zn_2L^2_2}$			
Bond length			
Zn(1)–N(18)	2.118(3)	Zn(1)–N(3)	2.133(2)
Zn(1)–N(5)	2.168(2)	Zn(1)–N(16)	2.180(3)
Zn(1)–N(20)	2.239(3)	Zn(1)–N(1)	2.264(2)
Zn(2)–N(13)	2.115(3)	Zn(2)–N(8)	2.129(3)
Zn(2)–N(15)	2.160(2)	Zn(2)–N(6)	2.177(2)
Zn(2)–N(10)	2.213(2)	Zn(2)–N(11)	2.246(3)

The ESI–MS spectrum of $\mathbf{ZnL^1}$ shows peaks at $m/z = 1227, 1127, 743, 644, 562$, and 500, which may be attributed to species $[\mathbf{Zn_2L^1_2} + \mathrm{ClO_4}]^+$, $[\mathbf{Zn_2L^1_2}]^+$, $[\mathbf{Zn_2L^1} + \mathrm{ClO_4} + \mathrm{OH}]^+$, $[\mathbf{Zn_2L^1} + \mathrm{OH}]^+$, $[\mathbf{ZnL^1}]^+$ and $[\mathbf{L^1} + \mathrm{H}]^+$. The peak at

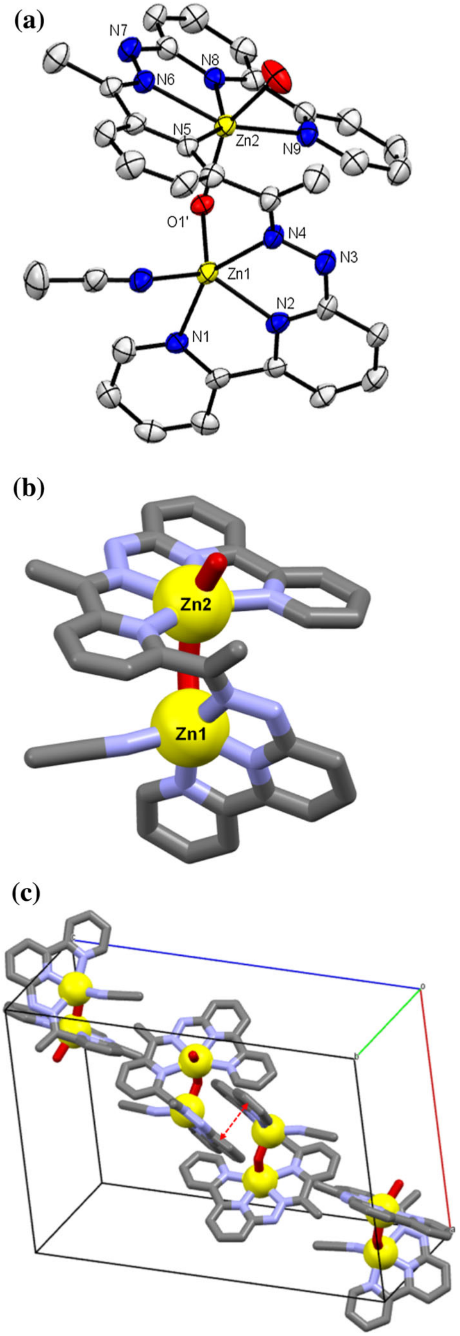

Fig. 2 The structure of the double helical complex cation of $\mathbf{Zn_2L^1}$, **a** ORTEP diagram, **b** representation of the helical structure, **c** representation of the intermolecular π–π interaction, $\mathrm{ClO_4}^-$ ions, solvent and hydrogen atoms are omitted for clarity

$m/z = 1227$ has been double checked to confirm a singly charged species, which indicates the presence of dinuclear complexes $[\mathbf{Zn_2L^1_2} + \mathrm{ClO_4}]^+$ in gaseous phase. The peak at $m/z = 1127$, was assigned to $[\mathbf{Zn_2L^1_2}]^+$ resulting from loss of an anion

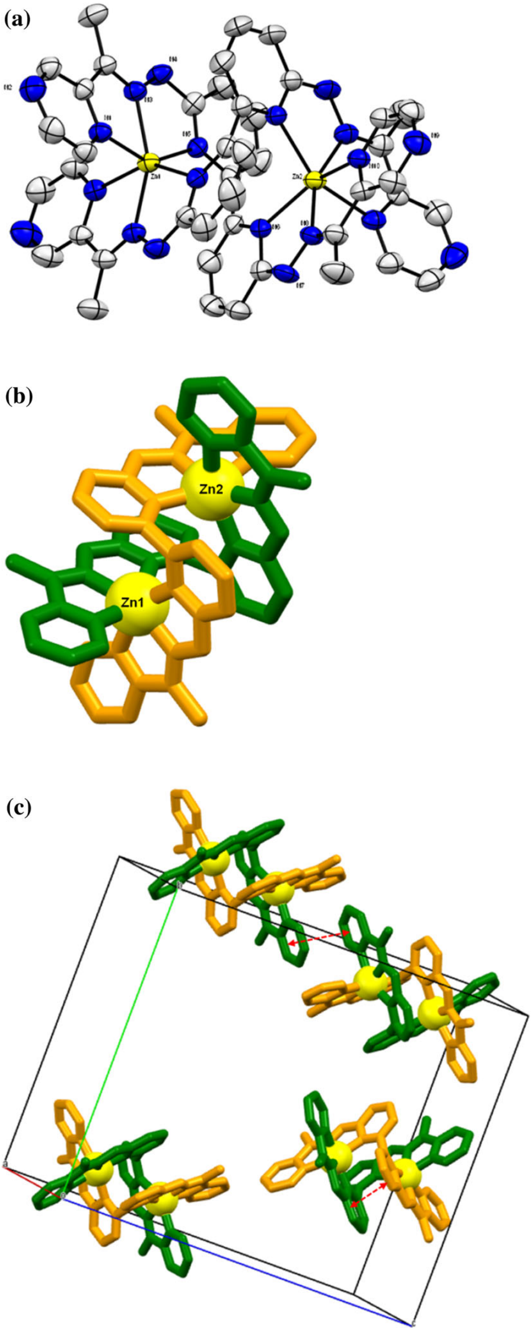

Fig. 3 The structure of the double helical complex cation of $\mathbf{Zn_2L^2_2}$, **a** ORTEP diagram, **b** representation of the double helical structure, **c** representation of the intermolecular and intramolecular π–π interaction, the $\mathrm{ClO_4}^-$ ions, solvent, and hydrogen atoms are omitted for clarity

Fig. 4 **a** The changes in UV/Vis spectra of 10^{-4} M $\mathbf{L^1}$ CH_3CN solution observed upon addition of▶ $Zn(ClO_4)_2$ to 10 equiv mole ratio. **b** Calculated spectra, **c** species distribution for complexation of Zn(II) with $\mathbf{L^1}$ by Specfit

and deprotonation of $[\mathbf{Zn_2L^1_2} + ClO_4]^+$ species. The ms/ms analysis shows that the signal of $[\mathbf{ZnL^1}]^+$ was derived from the decomposition of $[\mathbf{Zn_2L^1}]^+$. The single positive charge species results from the reduction of the charges by deprotonation of the NH groups. The simulated isotopic pattern is in good agreement with the measured spectrum. These results indicate the presence of dinuclear complexes. The intermediate species observed in the mass spectrum are consistent with those obtained in UV–Vis spectrometric titration modeling by the Specfit program.

X-ray structure

Zn_2L^1

Straw yellow crystals of $\mathbf{Zn_2L^1}$ were obtained by diffusion of toluene into a solution of the complex in CH_3CN. Selected bond lengths and angles are listed in Table 1. Crystallographic analysis reveals that a single-stranded helix structure is constructed by a twist ligand $\mathbf{L^1}$ surrounding the metal axis (Fig. 2). In addition, two zinc ions are bound to a bridge oxygen atom as a Zn–O–Zn structure. The helical structure is separated into two planes in a hinge-type, Zn(1) and one bipyridine in one plane, and Zn(2), pyridine, and another bipyridine in the second plane. The dihedral angle of these two planes is 74.18°. The Zn(1) ion bonds to two nitrogen atoms of bipyridine, acetonitrile, and oxygen in a trigonal bipyramidal coordination geometry. The Zn(2) ion occupies a distorted octahedral coordination geometry with two oxygen atoms in *trans* position and the four nitrogen atoms ($N_{bipyridine}$, $N_{hydrazone}$, and $N_{pyridine}$) in a plane. The distance between Zn(1) and Zn(2) was 3.4 Å, the angle of Zn(1)–O(1)–Zn(2) was 126.5°.

The distance between Zn(1) to the nitrogen atoms was around 1.909(4)–2.273(5) Å while Zn(2) to the nitrogen atoms was around 1.984(4)–2.335(5) Å. A distance of 3.7 Å was found, which implies that the intermolecular π–π stacking interaction between two bipyridine rings is from different helical units.

$Zn_2L^2_2$

Straw yellow crystals of $\mathbf{Zn_2L^2_2}$ were obtained by diffusion of toluene into a solution of the complex in CH_3CN. Selected bond lengths and angles are listed in Table 1. Crystallographic analysis revealed a double-stranded helix structure, which was formed with two zinc centers and two ligands (Fig. 3). The ligand wraps along the helical axis, which is formed by zinc ions. Each ligand provides three coordination sites for zinc in a twisting octahedral geometry by one pyridine of bipyridine unit, one hydrazone unit, and one pyrazine unit. Each pyridine of bipyridine unit is coordinated to a different zinc ion interlocking into a double helix structure. The dihedral angle between two pyridine rings of bipyridine is around 78°–85°. The Zn–Zn internal distance is 4.7 Å and implied no internal contact between the zinc(II)

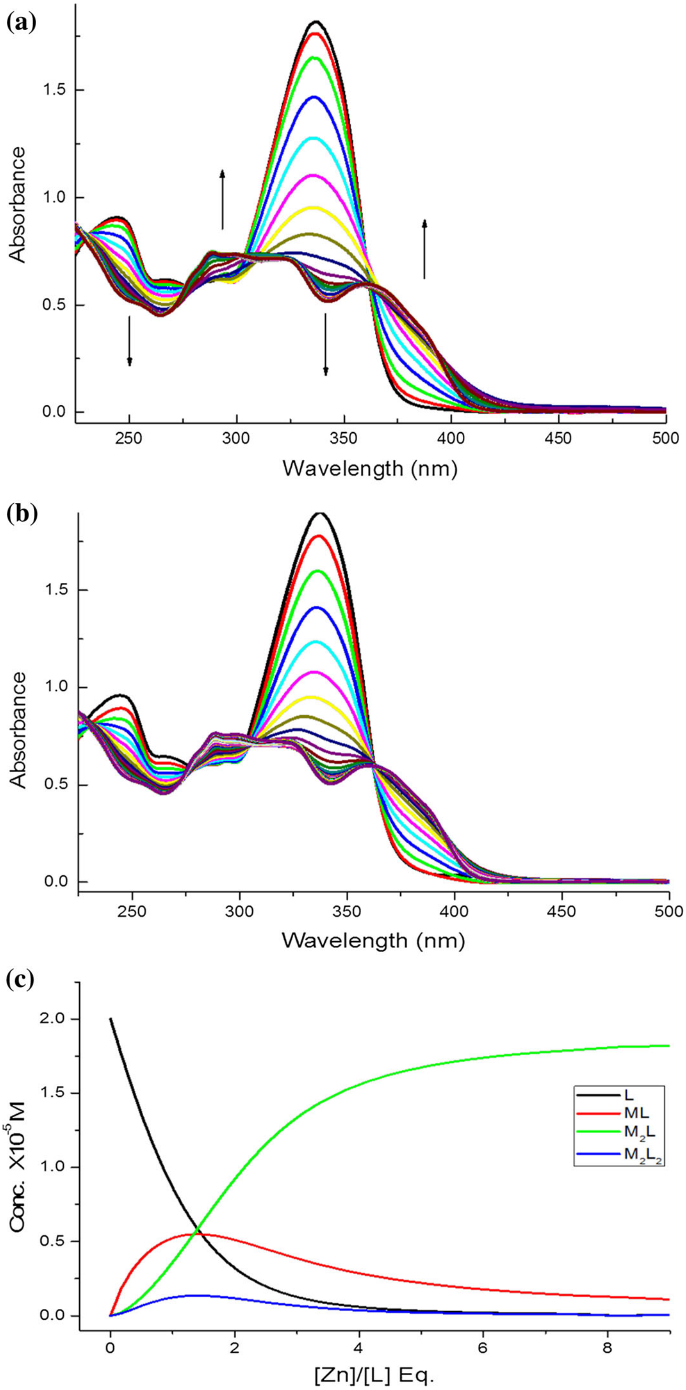
(a)
Absorbance
0.0
0.5
1.0
1.5
250
300
350
400
450
500
Wavelength (nm)
(b)
Absorbance
0.0
0.5
1.0
1.5
250
300
350
400
450
500
Wavelength (nm)
(c)
Conc. X10^{-5}M
0.0
0.5
1.0
1.5
2.0
0
2
4
6
8
[Zn]/[L] Eq.
L
ML
M$_2$L
M$_2$L$_2$

ions. The distances between pyridine nitrogen atoms and zinc ions are around 2.160(2) Å (Zn(2)–N(15)) and 2.180(3) Å (Zn(1)–N(16)). The distances between the hydrazone nitrogen atoms and zinc ions are around 2.115(3) Å (Zn(2)–N(13)) and 2.133(2) Å (Zn(1)–N(3)). The distances between pyrazine nitrogen atoms and copper ions are around 2.213(2) Å (Zn(2)–N(10)) and 2.264(2) Å (Zn(1)–N(1)). The N_{py}–Zn–N_{hyz} angles are around 146.02(9)° and 148.33(1)° when N_{py} and N_{hyz} are from the same strand, which is smaller when the N_{py} and N_{hyz} belong to different strands (around 86.12(9)° and 99.87(9)°). The distance between pyridine rings from one to the other ligand of about 3.5 Å suggests that there is intramolecular π–π stacking interaction between the two ligand strands. Similarly, a distance of about 3.7 Å between the pyrazine rings from different helical structures implied a weak intermolecular π–π stacking interaction between helical units (Fig. 3c) The height of the cylinder defined by the helical strand in the complex is about 11 Å, which was smaller than the dinickel(II) and dicopper(II) complexes in our previous report. No intermolecular interactions between perochlorate ions and helix strands were found, implying that the stacking interaction plays a key role in maintaining the helical conformation.

Spectrometric titration studies

The self-assembling process of $\mathbf{L^1}$ with $Zn(ClO_4)_2$ in CH_3CN was studied by UV–visible spectrometric titration (Fig. 4). The $\mathbf{L^1}$ absorption maxima occur at 245 and 338 nm (π–π*). Upon addition of Zn^{2+} to $\mathbf{L^1}$ to 0.5:1 ratio, the 338 nm peak decreases, and a new band appears at 385 nm, which can be attributed to coordination effects in the hydrazone moiety of $\mathbf{L^1}$. An isosbestic point at 363 nm was observed. Subsequent titration to 1:1 ratio of the two new additional isosbestic points at 231 and 271 nm were observed. These results revealed that $\mathbf{L^1}$ chelates to Zn^{2+} to form a stable $[\mathbf{ZnL^1}]^{2+}$ species. But the succeeding equilibrium formation of the double helical $[\mathbf{Zn_2L^1_2}]^{4+}$ species cannot be ruled out. Then, we propose a formation processes including $[\mathbf{Zn_2L^1_2}]^{4+}$ for an analysis of the stepwise characteristic in the formation of $[\mathbf{Zn_2L^1}]^{2+}$. The possibility for the formation of $[M_3L^1_2]^{6+}$ can be eliminated due to all coordination sites of the ligand being occupied by metal ions in its precursor, as found in solid state structure.

The SPECFIT/32 Global Analysis System, which performs a nonlinear best fit of the spectrometric data, was employed to obtain the thermodynamic parameters of the helicate formation processes. Figure 4 is the simulated UV–Vis spectra and partition curves of constitutions. The stability constants β_{ml} for each M_mL_l species in the proposed model are shown in Table 2. The calculated results highly conform to experimental data and satisfy the proposed model.

The calculated β_{ml} values and the overall stability constant of the complex $\mathbf{Zn_2L^1}$ are consistent with the similar process in analogous zinc complexes [37–39]. The presence of equilibrium intermediates fit well with those observed in the ESI–MS spectra in which no species containing more than two metal ions were found. The stepwise formation constants imply a slightly positive cooperative behavior for the formation of helicate.

Table 2 Stepwise formation equation and calculated formation constant

Stepwise formation equation	Formation constant
$Zn^{2+} + L^1 \rightleftharpoons [ZnL^1]^{2+}$	$\log \beta_{11} = 4.99$
$[ZnL^1]^{2+} + Zn^{2+} \rightleftharpoons [Zn_2L^1]^{4+}$	$\log \beta_{12} = 10.04 \pm 0.41$
$[Zn_2L^1]^{2+} + L^1 \rightleftharpoons [Zn_2L^1_2]^{4+}$	$\log \beta_{22} = 14.64 \pm 0.60$

Conclusion

The aim of this study was to obtain the self-assembled helicates between zinc(II) and polydentate ligands. We synthesized two ligands $\mathbf{L^1}$ and $\mathbf{L^2}$ based on the pyridinyl and hydrazone moieties, and which were designed with an opposite strategy. $\mathbf{L^1}$ has a relatively rigid structure design with the pyridine as a ligand core. $\mathbf{L^2}$ has a hinging-available design with the application of a bipyridine as a ligand core. The self-assembled dizinc(II) complexes were obtained by reaction of $\mathbf{L^1}$ and $\mathbf{L^2}$ with zinc(II) perchlorate in acetonitrile. The solid-state structure of single-stranded helicate $\mathbf{Zn_2L^1}$ and double-stranded helicate $\mathbf{Zn_2L^2_2}$ were confirmed by X-ray diffractometry. The mass spectrum and the spectrometric titration results of $\mathbf{L^1}$ implied the double-stranded helicate could be found at the solution state. The spectrometric titration results and the estimate of formation constants for the complexes also indicated that the formation of the helicate is driven by positive cooperativity.

Supporting information

Supplementary data of selected 1H and 13C NMR data associated with this article are available; the crystallographic data in CIF format have been deposited with the Cambridge Crystallographic Data Centre as supplementary publication numbers CCDC reference number CCDC 1037076 for $\mathbf{Zn_2L1}$ and 1032478 for $\mathbf{Zn_2L^2_2}$. Copies of the data can be obtained, free of charge, on application to CCDC, 12 Union Road, Cambridge CB2 1EZ, UK [fax: +44(0) 1223 336033 or email: deposit@ccdc.cam.ac.uk].

Acknowledgments This work was financially supported by Tamkang University and the Ministry of Science and Technology (NSC 97-2113-M-032-006). The authors thank Mr. Pierre LaPorte for reading the article.

References

1. U. Koert, M.M. Harding, J.-M. Lehn, Nature **346**, 339–342 (1990)
2. J.S. Lindsey, New J. Chem. **15**, 153–180 (1991)
3. J.-M. Lehn, *Supramolecular Chemistry-Concepts and Perspectives* (VCH, Weinheim, 1995)
4. C. Piguet, C. Edder, S. Rigault, G. Bernardinelli, J.-C. G. Bünzli, G. Hopfgartner, *J. Chem. Soc., Dalton Trans.* **22**, 3999-4006 (2000)
5. R. Ziessel, Coord. Chem. Rev. **195**, 201–217 (2001)
6. Y.-M. Legrand, A. Van Der Lee, M. Barboiu, Inorg. Chem. **46**, 9540–9547 (2007)
7. J.-M. Lehn, Chem. Soc. Rev. **36**, 151–160 (2007)

8. J.P. Sauvage, *Transition Metals in Supramolecular Chemistry* (Wiley, New Yoek, 2008)
9. E. Yashima, K. Maeda, Y. Furusho, Acc. Chem. Res. **41**, 1166–1180 (2008)
10. E. Yashima, K. Maeda, H. Iida, Y. Furusho, K. Nagai, Chem. Rev. **109**, 6102–6211 (2009)
11. D. Haldar, C. Schmuck, Chem. Soc. Rev. **38**, 363–371 (2009)
12. J.-M. Lehn, Angew. Chem. **100**, 91–116 (1988)
13. K. Zegelaar-Jaarsveld, G.A. Van DerMarel, J.H. Van Boom, Tetrahedron **48**, 10013–10148 (1992)
14. P.T. Corbett, J. Leclaire, L. Vial, K.R. West, J.-L. Wietor, J.K.M. Sanders, S. Otto, Chem. Rev. **106**, 3652–3711 (2006)
15. M. Nishijima, J.-W. Chang, C. Yang, G. Fukuhara, T. Mori, Y. Inoue, Res. Chem. Intermed. **39**, 371–383 (2013)
16. V. Amendola, L. Fabbrizzi, C. Mangano, P. Pallavicini, E. Roboli, M. Zema, Inorg. Chem. **39**, 5803–5806 (2000)
17. V. Amendola, L. Fabbrizzi, P. Pallavicini, E. Sartirana, A. Taglietti, Inorg. Chem. **42**, 1632–1636 (2003)
18. T. Ghosh, S. Pal, Inorg. Chim. Acta **363**, 3632–3636 (2010)
19. R.-F. Song, Y.-Y. Sun, J. Yang, X.-Y. Yang, J. Inorg. Organomet. Polym. **21**, 237–243 (2011)
20. M.T. Youinou, R. Ziessel, J.-M. Lehn, Inorg. Chem. **30**, 2144–2148 (1991)
21. A.-M. Stadler, N. Kyritsakas, G. Vaughan, J.-M. Lehn, Chem. Eur. J. **13**, 59–68 (2007)
22. F.A. Cotton, G. Wilkinson, *Advanced Inorganic Chemistry* (Wiley, New York, 1988)
23. D.S. Auld, Biometals **14**, 271–313 (2001)
24. J.M. Berg, Y. Shi, Science **271**, 1081–1085 (1996)
25. L.A. Finney, T.V. O'Halloran, Science **300**, 931–936 (2003)
26. N.C. Lim, H.C. Freake, C. Brückner, Chem. Eur. J. **11**, 38–49 (2005)
27. Y. Wu, J.-C. Liu, J. Cao, R.-Z. Li, N.-Z. Jin, Res. Chem. Intermed. (2014). doi:10.1007/s11164-014-1781-8
28. H.-C. Kao, Y.-C. Wang, W.-J. Wang, J. Chin. Chem. Soc. **57**, 876–882 (2010)
29. H.-C. Kao, Y.-C. Wang, W.-J. Wang, J. Chin. Chem. Soc. **59**, 934–939 (2012)
30. G.M. Sheldrick, *SHELX-97, Programs for Crystal Structure Solution and Refinement* (University of Göttingen, Göttingen, 1997)
31. SADABS. Version 2007/2. G. M. Sheldrick, (Bruker AXS Inc. Madison, Wisconsin, USA, 1997)
32. R. Binstead, A. D. Zuberbuhler, SPECFIT Global Analysis System, 2.10 edn. (Spectrum Software Associates: Chapel Hill, NC 27515, 1998)
33. E.R. Malinowski, D.G. Howery, *Factor Analysis in Chemistry* (Wiley, New York, 1980)
34. H. Gampp, M. Maeder, C.J. Meyer, A.D. Zuberbuhler, Talanta **23**, 1133–1139 (1985)
35. H. Gampp, M. Maeder, C.J. Meyer, A.D. Zuberbuhler, Talanta **33**, 943–951 (1986)
36. S. Anderson, E. C. Constable, K. R. Seddon, J. E. Turp, J. E. Baggott, M. J. Pilling, *J. Chem. Soc., Dalton Trans.* **11**, 2247-2261 (1985)
37. C. Piguet, B. Bocquet, A. Quattropani, J. Am. Chem. Soc. **114**, 7440–7451 (1992)
38. C. Piguet, B. Bocquet, A. Quattropani, J. Am. Chem. Soc. **116**, 9092–9102 (1994)
39. J. Hamacek, S. Blanc, M. Elhabiri, E. Leize, A.V. Dorsselaer, C. Piguet, A.M. Albrecht-Gary, J. Am. Chem. Soc. **125**, 1541–1550 (2003)